

# Quasiharmonic approximation for a double Morse-type local potential model: Application to a $\text{KH}_2\text{PO}_4$ -type phase diagram

S. E. Mkam Tchouobiap\* and H. Mashiyama

*Graduate School of Science and Engineering, Yamaguchi University, Yamaguchi 753-8512, Japan*

(Received 14 January 2007; revised manuscript received 10 April 2007; published 2 July 2007)

In order to describe a structural phase transition at low temperature, a quantum particle within a local potential is considered. According to the general formalism presented by Salje *et al.* [*Z. Phys. B* **82**, 399 (1991)], a quasiharmonic approximation is applied to the local potential and the interaction is replaced by the mean field one. The rigorous effective potential is reduced from a double Morse-type potential. The order parameter, the variance, and the effective soft frequency are given by analytic equations with potential parameters. As an application, a molecular motion of  $\text{H}_2\text{PO}_4$  in KDP is considered and the disappearance of the ordered phase at low temperature under high pressure is discussed. The difference between KDP and DKDP crystals are described successfully by the presented model.

DOI: [10.1103/PhysRevB.76.014101](https://doi.org/10.1103/PhysRevB.76.014101)

PACS number(s): 64.60.-i, 63.70.+h, 77.80.Bh, 77.84.Fa

## I. INTRODUCTION

Although the mechanism of structural phase transitions in crystals and particularly in ferroelectric materials has been at the heart of many extensive studies for several decades, there are still many unsolved questions which continue to warrant and receive further attention. For example, the importance of switchable macroscopic polarization which characterize ferroelectric materials stems not only from technological considerations, but also from a fundamental interest in understanding the structural phase transitions and symmetry breaking involved.<sup>1</sup> Thus, structural transition has an important influence on their thermodynamic stability. So far, one of the important clues in understanding the physical mechanism of structural transitions is the behavior of the local microscopic structure as a function of temperature, pressure, and composition.<sup>2-7</sup>

As it is well known, conventionally, two categories of structural phase transitions are considered in ferroelectrics: displacive transitions in which the local structural distortions follow the behavior of the order parameter and vanish in the high symmetry phase and order-disorder transitions in which local distortions persist deep into the high symmetry phase in spite of the fact that the average distortion is zero.<sup>8-11</sup> Correspondingly, the quantum effect of polarization fluctuation is described somewhat differently. According to the character of the motion, in displacive ferroelectrics, the spontaneous polarization arises as a result of freezing of lattice vibrations, which from the dynamical response are characterized by soft modes, with diminishing frequency as the transition is approached.<sup>12</sup> In this case, occurrence of ferroelectricity has been usually discussed by the anharmonic lattice vibrations.<sup>1,13,14</sup> On the other hand, an order-disorder system like  $\text{NaNO}_2$  is composed of permanent electric dipoles, which by alignment, yields spontaneous polarization. Thus, the ferroelectricity arises from the cooperative arrangement of ions or permanent dipoles. Here, the local potential for the order parameter has the multiminimum structure. Hence, the variable associated with the polarization is considered to take several discrete values, effectively expressed by “spin variable.” The motion is then often described by the pseudospins

through the Ising model or the stochastic model like those expressed in terms of  $2 \times 2$  Pauli spin operators.<sup>1,15</sup>

In order to investigate them, several simple models and formalisms have been proposed and analyzed, as Landau theory, soft modes concept, molecular field approximation (MFA), self-consistent phonon approximation (SPA), or quasiharmonic approximation for which the important tool is to calculate the Gibbs free energy, whereas the quasiharmonic approximation, which represents the system through the renormalization process of the anharmonic part, by a quasiharmonic system with the renormalized frequency, was at first only used for displacive systems.

Even though these two theoretical mechanisms of ferroelectricity are physically transparent and convenient in a sense, it has turned out that many ferroelectric substances do not allow necessarily typical behavior in either case and are now exhibited features common to them, i.e., they may be in general rather located in the “intermediate” states, exhibiting both features concurrently. Thus, the displacive and order-disorder concepts appear now gradually and are not conflicting. Since many models were proposed to study not only the order-disorder but also the displacive ferroelectrics simultaneously. These models were taken into account using different concepts like the unified anharmonic oscillator model by Onodera,<sup>16</sup> or the simple microscopic model in terms of local normal coordinates by Salje *et al.*,<sup>14</sup> which was later reformulated and introduced by Pérez-Mato and Salje;<sup>17</sup> for most of them, their starting point is the anharmonic potential.

Furthermore, for example, potassium dihydrogen phosphate  $\text{KH}_2\text{PO}_4$  (KDP) family is one of the typical hydrogen-bonded ferroelectric crystals and has been most extensively studied. The structural moiety consists of alkaline metal, tetrahedral ion, and a hydrogen bond to connect two tetrahedra. Then, KDP belongs to a family of ferroelectric crystals where molecular units are linked by hydrogen bonds. The ferroelectricity may be connected to proton off-center ordering in the bonds.<sup>18-20</sup> Since ferroelectricity of KDP was discovered below  $T_c = 123$  K in 1935,<sup>18</sup> a lot of experimental and theoretical studies have been carried out intensively on the mechanism of ferroelectric phase transition. The earliest statistical mechanical model introduced by Slater to describe

the ferroelectric phase transition and more recently crystal lattice dynamics measurements have suggested the order-disorder mechanism of phase transition.<sup>2,20,21</sup> Also, one of the important characteristics of the KDP family is its huge isotope effect of  $T_c$  known upon deuteration. After the discovery of a remarkable isotope effect:  $T_c$  rises about 100 K if the proton is replaced by deuteron  $\text{KD}_2\text{PO}_4$  (DKDP), which could not be explained by the Slater model, the proton tunneling model proposed by Blinc,<sup>22</sup> the earliest model used to explain the isotope effect, predicted the displacive type of phase transition. According to this model, the tunneling frequency was expected to slow down near  $T_c$ .

Although the origin of the isotope effect has been mostly understood in terms of the above quantum tunneling model, modified later by Kobayashi who included the coupling between proton motion and the  $\text{K-PO}_4$  dynamics,<sup>23</sup> it is still controversial, and it was recognized that the pure protonic models are not sufficient to explain ferroelectric properties of KDP. In addition, theoretical investigation of KDP-type phase diagram was performed by Blinc,<sup>22</sup> and recently by Mashiyama,<sup>24</sup> whose results, using linear response theory and mean-field approximation, have reported that the two level system is essential both for KDP and DKDP. But, the real nature of the ferroelectric phase transition and the isotope effect on  $T_c$  for  $\text{H} \rightarrow \text{D}$  exchange in  $\text{KH}_2\text{PO}_4$  or KDP-type ferroelectric has not been fully explained. According to the above, the order-disorder model can be also analyzed but determining its Gibbs free energy and the real potentials in the crystals are not necessarily expressible by simple form.<sup>13,24–29</sup> There are basically two approaches to calculate Gibbs free energy. One approach uses molecular dynamics or Monte Carlo methods to sample the configuration space and then calculate the Gibbs free energy from ensemble average. The other approach uses quasiharmonic approximation to estimate the free energy contribution due to ion motion.

In regard to the above, and according to recent developments, the modelization of the substrate potential by a polynomial function appears as a too simplified approximation. For example, it is established that under variation of some physical parameters such as the temperature and pressure, certain physical systems may undergo changes which are either shape distortions, variations of crystalline structures or conformational changes.<sup>24,27,30</sup> Thus, quantitative and qualitative thermodynamic analysis of most ferroelectric materials cannot be studied efficiently within the standard approach of rigid lattices. Also when the barrier height of the double-well potential, which is a factor of particular importance, cannot be varied. This is the case in rigid potentials, so it appears as a drastic restriction in modeling a large amount of the physical systems, as for example, the hydrogen-bonded ferroelectrics.<sup>24,27,31</sup>

In the present paper, employing the quasiharmonic approximation proposed by Salje *et al.*,<sup>14</sup> we give an analytical description of the structural phase transitions in a nonlinear simple microscopic model in which the substrate potential is a deformable double-well potential of double Morse type.<sup>17,24</sup> The interparticle potential is described by an appropriate harmonic interaction potential that reflects the change in the electronic distribution of the sites. We develop a mean-field treatment for this model to analyze structural phase

transitions and examine how the disparities in the single-site potential are manifested in the thermodynamic and responses of the systems to external influences. The particular one developed here is a modification and extension of a theory originally introduced by Thomas,<sup>14,32</sup> to analyze second-order and tricritical ones.

The organization of the paper is as follows. In Sec. II, we present the model Hamiltonian. In Sec. III, mean-field theory is used to derive the analytical expression of the free-energy and the mean-field equations are analyzed. In this connection, the origin of the thermodynamic saturation is presented, where the quantum saturation and fluctuation of order parameter have been recognized and have an important influence on the behavior of the systems. Also, the influence of the quantum effect was analyzed. In Sec. IV, using a plausible assumption that the potential splitting  $d$  and the interaction strength  $v$  are pressure dependent, the model and theory are applied to the KDP-type crystals. Their corresponding calculated pressure-temperature phase diagrams have been investigated and analyzed, and the influence of the potential splitting  $d$  and the interaction parameter  $v$  on the transition temperature has been investigated. The numerical calculated values of the critical transition temperatures and pressures for KDP and DKDP are given. It appears that phase transitions in KDP and DKDP are closed to the displacive limit and nearly tricritical. We devote Sec. V to a summary of the results and discussions.

## II. MODEL HAMILTONIAN

Many two- or three-dimensional crystal systems can be regarded as a compound system of multiply linked one-dimensional chains.<sup>1,8,14,17,24,33</sup> Then, in order to investigate the quantum saturation of the spontaneous polarization in ferroelectric materials, study the quantum fluctuation of the order parameter in the structural phase transition and the pressure dependence of the transition temperatures in ferroelectrics, ferroelastics, and related materials, Pérez-Mato and Salje introduced the following generalized simple microscopic model, which might undergo structural phase transitions, with the model Hamiltonian,<sup>17,33</sup>

$$H = \sum_l \left( \frac{1}{2m} p_l^2 + V(Q_l) \right) + \frac{1}{4} \sum_{ll'} v_{ll'} (Q_l - Q_{l'})^2, \quad (1)$$

where  $m$  is the effective mass associated with the local normal coordinates of the ferroelectric mode  $Q_l$ ,  $p_l$  are the conjugate momenta, and  $v_{ll'}$  are the interaction constants.

The local double-well potential  $V(Q_l)$  has been given by quartic form  $V(Q_l) = (-2Q_l^2 + Q_l^4)E_0$ .<sup>17,33</sup> Here, the instability of the ferroelectric soft mode is attributed to the harmonic attractive Coulomb forces acting between different atoms which is modeled by the force constant  $-2Q_l^2 E_0 < 0$ , and the stabilization in the paraelectric and ferroelectric phases is achieved via the one-site fourth-order coupling constant  $Q_l^4 E_0 > 0$ . Thus, the one-site local potential is therefore that of a particle moving in a double minimum potential.

Also, the various physical parameters are intuitive. This model follows from more general physical ferroelectric mod-

els of which the spontaneous polarization  $P$  of the ferroelectrics is equivalent to the order parameter  $Q$ . The model also captures the polar origin and the essential three dimensionality of the local field responsible for the instability and the static displacements of the ions. The microscopic reasoning for this potential is due to the local instability of the chain environment so that their nonlinearity must not be ignored. For example, among a large number of known ferroelectric crystals, those containing hydrogen bonds which appear when the hydrogen atom is found to be a neighbor of a strongly electronegative atom (oxygen, nitrogen, fluorine, chlorine, etc.), the most thoroughly studied crystals are those of  $\text{KH}_2\text{PO}_4$  (KDP).

In most cases, the potential energy of the proton of the hydrogen bond is described by a curve with two minima separated by a potential barrier. Although the physical origin of the double-well substrate local potential is well known, its modelization by a polynomial function of quartic-type is still an over-simplified approximation since the minima of this double-well potential as well as the height of its barrier are fixed. For instance, phase transitions in ferroelectric systems are usually connected with the rearrangements of a few atoms in the unit cell whereas the positions of all others remain almost unchanged.

In the hydrogen-bonded systems and particularly ferroelectrics such as  $\text{KH}_2\text{PO}_4$  or  $\text{KD}_2\text{PO}_4$  (KDP-type crystals), it is now well recognized that the variation of distance between the heavy ions that surround a proton modulates the double-well experienced by the protons.<sup>24,27,34</sup> Then, insights gained from the earliest double-well potential model, i.e., the  $\phi^4$ , have reached saturation points owing to several shortcomings. For instance the rigidity of this model prevents one from getting further into theoretical investigations as for example, taking analytically into account the possibility to shift the potential minima and hump so to adjust the model to a desired context. In this context, a few families of deformable double-well potentials have appeared in the literature.<sup>24–29</sup>

Because it is widely accepted that a Morse potential is successful for a covalent-bonding atom, we consider the double Morse substrate potential which has been considered frequently,<sup>13,24–26,31</sup>

$$V(Q_l) = 2D[e^{-2ad} \cosh(2aQ_l) - 2e^{-ad} \cosh(aQ_l)], \quad (2)$$

which is formed by superposing back-to-back two (left and right) identical Morse potentials

$$V^L(Q_l) = D\{\exp[-2a(Q_l + d)] - 2 \exp[-a(Q_l + d)]\} \quad (3)$$

and

$$V^R(Q_l) = D\{\exp[2a(Q_l - d)] - 2 \exp[a(Q_l - d)]\}; \quad (4)$$

where  $D$ ,  $a$ , and  $d$  are the parameters proper to the initial Morse function. For the case of proton in KDP,  $2d$  represents the splitting between the two equivalent minimum of the proton potential, and is related to the O-O distance  $R$  and the O-H distance  $r_0$  by the following relation,

$$2d = R - 2r_0. \quad (5)$$

The local potential has an important property: All the characteristic points of the potential vary at the same time.

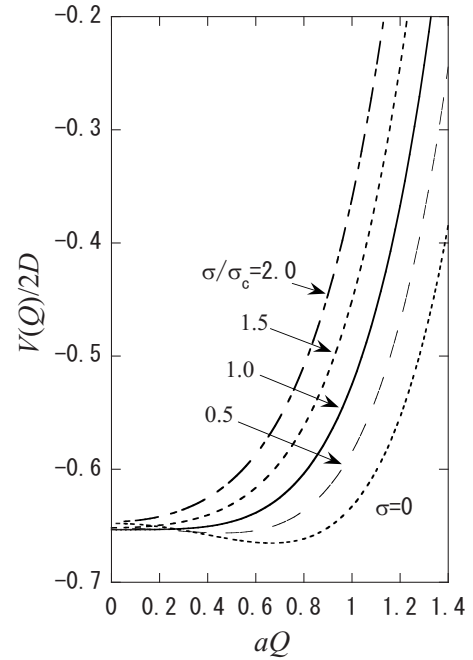


FIG. 1. Bare two-Morse potential ( $\sigma=0$ ) and the effective potentials for given  $\sigma/\sigma_c$  between 0.5 to 2, with parameters  $a=3.0$  and  $d=0.3$ . The potential is scaled by  $2D$ .

Then, as  $d$  increases, the barrier height of the double-well continuously increases and the minima of the potential also vary continuously with  $d$ . Moreover, the barrier between the two wells is much lower when the two (neighboring) minima approach each other. This is an essential ingredient, which allows an easier migration of the proton, when the bond is stronger.<sup>31</sup> Also this is an example of nonpolynomial double-well potential which is infinitely differentiable and which approaches the harmonic potential at large distances, and with much stronger anharmonicity than the  $\phi^4$  chain.<sup>13,24–29,31</sup>

The positions of the double minima of  $V(Q_l)$  are given by

$$\pm \Delta Q = \frac{1}{a} \ln \left[ \frac{1}{2} e^{ad} + \left( \frac{1}{4} e^{2ad} - 1 \right)^{1/2} \right]. \quad (6)$$

It is to be noted that the quantity  $d$  must be larger than  $\ln 2/a$  in order for  $V(Q_l)$  to form a double well.

The value

$$\Delta V = D(2e^{-ad} - 1)^2 \quad (7)$$

corresponds to the height of the potential barrier between two degenerated minima of the local potential located at the varying points  $Q_{1,2} = \pm \Delta Q$ . The double Morse potential has an extremely steep side wall and a relatively flat panlike bottom, whose sketches of the bare potential and the effective potentials for several values of variance  $\sigma$ , which is defined by (14) in the next section, are shown in Fig. 1. Another interesting feature of this model is that contrary to the others aforementioned deformable double-well potentials which do not allow one to proceed far enough in theoretical analysis, particularly in discrete systems, its quantum coun-

terpart belongs to the class of the so-called quasireactly solvable models.<sup>24,35</sup>

### III. FORMALISM

In order to investigate the structural properties of ferroelectric phase transitions over a wide temperature interval around the transition temperature, we present here a derivation of the quantum-mechanical mean-field treatment,<sup>14</sup> which is accepted widely to be appropriate for ferroelectrics. The type of transition is determined by the wave number  $q_0$  at which the Fourier transform of the interaction  $v_{ll'}$  assumes its maximum value  $v=v_{q_0}>0$ . For example,  $q_0=0$  is a ferrodistorptive transition with  $\langle Q_l \rangle = Q$  and for  $q_0=\text{reciprocal lattice vector}/2$ , we have an antiferrodistorptive transition with  $\langle Q_l \rangle = \pm Q$ .<sup>14</sup>

In the context of this work we consider  $q_0=0$  for the local potential of Eq. (2) at each lattice site. Also, the following parameters are now defined for convenience:

$$v = \sum_{l'} v_{ll'},$$

$$\varepsilon_0 = \frac{\Delta V}{v(\Delta Q)^2} = \frac{D}{v} \left( \frac{a(2e^{-ad} - 1)}{\ln(1/2)[e^{ad} + (e^{2ad} - 4)^{1/2}]} \right)^2. \quad (8)$$

The parameter  $\varepsilon_0$  describes the nature of the transition:  $\varepsilon_0 \rightarrow 0$  corresponds to the displacive limit, while  $\varepsilon_0 \rightarrow \infty$  denotes the order-disorder Ising limit. The former case means that the height of the potential barrier in the double-well local potential Eq. (2) is small as compared with the interaction energy between nearest-neighbors (the case of strong coupling between nearest-neighbors relative to the energy barrier of the double-well potential).<sup>5,8</sup> It is important to note that the saturation behavior at low temperature is driven by thermodynamic effects, and not because the order parameter has reached some maximum value, which can never be exceeded.<sup>33,36,37</sup>

According to the fact that the saturation temperature for the order parameter is expected to be similar to the saturation temperature of the bare soft mode, which depends on its bare frequency, the bare saturation temperature is given by

$$\theta_s = \frac{1}{2} \frac{\hbar}{k_B} \left( \frac{v}{m} \right)^{1/2}, \quad (9)$$

which shows the atomic mass dependency of quantum effects.<sup>17,33</sup>  $\theta_s$  also characterizes the temperature of the cross-over between classical and quantum mechanical behavior and it is related to the ground state energy of the quantum particle oscillator.

We now derive the Gibbs free energy in a mean-field approximation (MFA) given by

$$F = \text{Tr}(\rho^{tr} H + k_B T \rho^{tr} \ln \rho^{tr}), \quad (10)$$

with a trial density matrix of the entire model<sup>32</sup>

$$\rho^{tr} = \frac{1}{Z^{tr}} \exp\left(\frac{-H^{tr}}{k_B T}\right), \quad (11)$$

where the trial Hamiltonian  $H^{tr}$  is a sum over effective single-site Hamiltonians,

$$H^{tr} = \sum_l \left( \frac{1}{2m} p_l^2 + \frac{1}{2} m \Omega^2 (Q_l - \langle Q_l \rangle)^2 \right). \quad (12)$$

The partition function for the trial Hamiltonian is given by

$$Z^{tr} = \text{Tr} \left[ \exp\left(\frac{-H^{tr}}{k_B T}\right) \right] = \left[ 2 \sinh\left(\frac{\hbar \Omega}{2k_B T}\right) \right]^{-N}. \quad (13)$$

Since  $H^{tr}$  is quadratic, all expectation values may be expressed in terms of  $Q = \langle Q_l \rangle$  and the variance

$$\sigma = \langle (Q_l - \langle Q_l \rangle)^2 \rangle = \langle (\delta Q_l)^2 \rangle, \quad (14)$$

where  $\langle \dots \rangle$  indicate the thermal average. Two variational parameters per site, an effective single-site frequency  $\Omega$  (same at each site) and the order parameter  $Q$  must be determined by minimizing the free energy of the system with respect to these parameters.

Calculating the average of the local single-site potential is tedious but we obtain

$$\langle V(Q_l) \rangle = 2D \left[ e^{-2ad} \exp(2a^2 \sigma) \cosh(2aQ) - 2e^{-ad} \exp\left(\frac{a^2 \sigma}{2}\right) \cosh(aQ) \right]. \quad (15)$$

Using Eqs. (10)–(15), one finds for the free energy the following resulting expression:

$$F = N k_B T \ln \left[ 2 \sinh\left(\frac{\hbar \Omega}{2k_B T}\right) \right] + N \left( \langle V(Q_l) \rangle + \frac{1}{2} v \sigma - \frac{1}{2} m \Omega^2 \sigma \right), \quad (16)$$

where  $N$  is the total single-site particle number. We note that minimizing  $F$  with respect to variational parameters  $Q$  and  $\Omega$ , produces the following mean-field equations:

$$\left[ 2e^{-ad} \exp(2a^2 \sigma) \cosh(aQ) - \exp\left(\frac{a^2 \sigma}{2}\right) \right] \sinh(aQ) = 0, \quad (17)$$

$$m \Omega^2 = v + 4a^2 D \left[ 2e^{-2ad} \exp(2a^2 \sigma) \cosh(2aQ) - e^{-ad} \exp\left(\frac{1}{2} a^2 \sigma\right) \cosh(aQ) \right]. \quad (18)$$

Equations (17) and (18) are the state equations for the thermodynamic limit of the model in the quasiharmonic approximation and must be solved self-consistently. The temperature-dependent Einstein frequency (effective frequency)  $\Omega$  and the quantum-mechanical expression of the variance  $\sigma$  for the soft modes are related by

$$\sigma = \frac{\hbar}{2m\Omega} \coth\left(\frac{\hbar \Omega}{2k_B T}\right). \quad (19)$$

It can be easily seen that Eqs. (17) and (18) possess two sets of solutions, which along with Eq. (16) for the free energy, constitute the mean-field description of the statistical mechanics of the system. The simpler one, with  $Q=0$ , is an undisplaced solution and corresponds to the symmetrical phase (paraelectric phase), while the other solution which is a displaced one ( $Q \neq 0$ ), corresponds to the nonsymmetrical phase (ferroelectric phase). The variance at the stability-limit points (critical points) characterized by vanishing order parameter is found from Eq. (17), by letting  $Q \rightarrow 0$ ,

$$\sigma_c = \frac{2}{3a^2}[ad - \ln(2)], \quad (20)$$

which is independent of the displacive degree  $\epsilon_0$ .

According to the third law of thermodynamics, which implies that absolute zero temperature cannot be attained (no entropy change, and hence no order parameter change occurs in the limit  $T \rightarrow 0$ ), the spontaneous polarization of ferroelectrics becomes temperature independent below a characteristic temperature ( $T \ll \theta_s$ ) due to freezing of fluctuation degree of freedom. Then, as the order parameter  $Q$  in structural phase transitions is usually a monotonous function of entropy with  $\frac{dS}{dQ} \neq 0$ , a direct consequence of this is that  $\partial Q / \partial T \rightarrow 0$  as  $T \rightarrow 0$ , i.e., the temperature evolution of order parameter saturates at low temperatures. Also, this saturation behavior is driven by thermodynamic effects.<sup>33,36,37</sup> Then, taking  $\theta_s$  as a measure of the temperature below which the temperature dependence of the order parameter is dominated by quantum mechanical effects,<sup>30</sup> the phase transition occurs at  $T_c$  when

$$\sigma(T_c) = \frac{k_B \theta_s}{v} \coth\left(\frac{\theta_s}{T_c}\right) = \sigma_c, \quad (21)$$

if the transition is a second-order one. In (21), the transition is characterized by two temperatures,  $\theta_s$  and  $T_c$ . Traditionally, studies of phase transitions have focused on  $T_c$ . However, determinations of  $\theta_s$  may also yield useful insights into the behavior of phase transitions. If  $T_c$  and  $\theta_s$  are known for the given self-potential system, the interaction parameter  $v$  can be estimated from (21). Also, phase transitions are suppressed by quantum fluctuations if

$$\frac{k_B \theta_s}{v} > \sigma_c. \quad (22)$$

Thus, for the order parameter in the ordered phase, one obtains

$$Q = \frac{1}{a} \cosh^{-1} \left[ \exp \left( \frac{3a^2}{2} (\sigma_c - \sigma) \right) \right], \quad (23)$$

and the correction of the transition temperature due to quantum effects (influences) is given by

$$T_c = T_c^{(\theta_s=0)} \frac{k_B \theta_s}{v \sigma_c} \coth^{-1} \left( \frac{v \sigma_c}{k_B \theta_s} \right), \quad (24)$$

where the classical transition temperature is defined by  $T_c^{(\theta_s=0)} = v \sigma_c / k_B$ . It is also the temperature of continuously vanishing order parameter in the displacive limit and is independent of the displacive degree  $\epsilon_0$ .

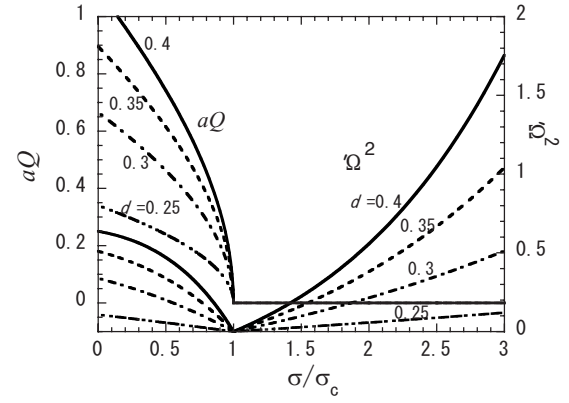


FIG. 2. Spontaneous displacement  $Q$  and squared effective frequency  $\Omega^2$  for  $d=0.25, 0.3, 0.35$ , and  $0.4$ , with parameter  $a=3$ . The squared frequency  $\Omega^2$  represents  $[(\Omega/\Omega_0)^2 - 1]/\Delta$  from Eq. (26).

An important point is that, unlike  $T_c$ , it seems that  $\theta_s$  is not greatly altered by chemical doping, or the application of external fields.<sup>36</sup> In order to improve well our theoretical understanding of the mechanism of phase transitions, and investigate the quantum effects, the following self-consistency condition for  $\sigma$  in the ordered phase, which follows from Eqs. (19) and (18), respectively, is obtained

$$\sigma = \sigma_c \frac{\Omega_0}{\Omega} \eta \coth\left(\frac{\Omega \eta}{\Omega_0 \chi}\right), \quad (25)$$

$$\Omega^2 = \Omega_0^2 \{1 + \Delta [\exp(-a^2 \sigma) - 4e^{-2ad} \exp(2a^2 \sigma)]\}, \quad (26)$$

where the following parameters are introduced:

$$\Omega_0 = (v/m)^{1/2}, \quad \eta = \hbar / (2m\Omega_0 \sigma_c),$$

$$\chi = k_B T / (m\Omega_0^2 \sigma_c), \quad \Delta = 2a^2 D / (m\Omega_0^2). \quad (27)$$

Here  $\chi$  is a normalized temperature and  $\Omega_0$  is the displacive limit Einstein frequency. In the fully dispersive limit,  $\Omega_0$  may be visualized as a characteristic frequency which is the Einstein mode frequency for oscillations with the intersite interactions. Dimensionless parameters  $\Delta$  and  $\eta$  are proportional to the distance from the displacive limit and a measure of the quantum influence (quantum-effect magnitude), respectively. It is important to remark here that  $\eta$  originates not in the tunneling motion but in the quantum vibration (such as zero-point energy) and  $\eta=0$  yields the classical result.<sup>7,14,33</sup>

In order to obtain the order parameter, we must solve (23), (25), and (26) self-consistently. The following parameters are considered concretely,  $a=3 \text{ \AA}^{-1}$ ,  $d=0.25-0.4 \text{ \AA}$ ,  $D=0.05-0.2 \text{ eV/\AA}^2$ . For a different set of values of the potential splitting parameter  $d$ , the spontaneous displacement  $Q$  and the square of the effective frequency are plotted in Fig. 2 as function of variance  $\sigma/\sigma_c$ , showing the presence of Einstein modes with relatively flat dispersion of the soft mode as  $d$  decreases. In the figure,  $[(\Omega/\Omega_0)^2 - 1]/\Delta$  is displayed by the right vertical axis. According to Fig. 2, the extremum value of the effective frequency shifts to the higher values of  $\sigma$  as  $d$  increases. Thus, changes in  $d$  are crucial to the existence regime of phases. The higher  $d$  becomes, the more the

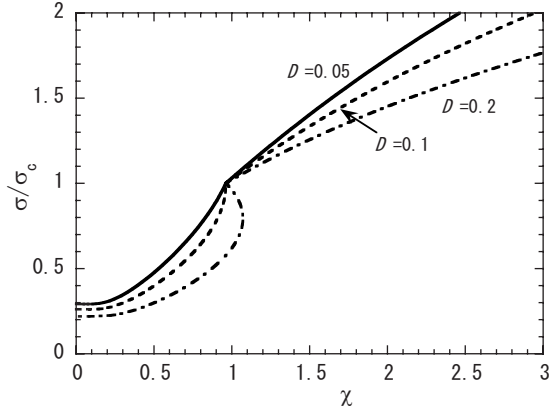


FIG. 3. Relation between the reduced variance  $\sigma/\sigma_c$  and the normalized temperature  $\chi$  for  $D=0.05, 0.1$ , and  $0.2$  eV, with parameters  $a=3 \text{ \AA}^{-1}$ ,  $d=0.3 \text{ \AA}$ ,  $v=1.0 \text{ eV/\AA}^2$ , and  $m=50$  amu.

quantum fluctuations dominate the dynamics. Also, Fig. 2 shows that the order parameter depends strongly on the potential splitting  $d$  and decreases with  $d$ . When  $\sigma/\sigma_c < 1$ , the spontaneous displacement  $Q \neq 0$ , and decreases slowly to zero as  $\sigma$  increases. Here is the main characteristic of the displaced solution, which corresponds to the ferroelectric phase. When  $\sigma/\sigma_c > 1$ , the spontaneous displacement is always equal to zero regardless of the variance value for the soft modes. Such a situation characterizes the symmetric disposition of the model, which attends to the undisplaced solution characteristic of the paraelectric phase. Hereafter this transition is referred to as a ferroelectric transition.

In order to understand the ferroelectric instability, we focus on the relationship between the variance and the normalized temperature  $\chi$ . This is done by solving (25) and (26) simultaneously: the numerical results are displayed in Fig. 3 for three different values of the dissociation energy  $D$ . The models parameters are  $a=3 \text{ \AA}^{-1}$  and  $d=0.3 \text{ \AA}$ ,  $v=1.0 \text{ eV/\AA}^2$ , and  $m=50$  amu. It appears for the evolution of  $\sigma$  against  $\chi$  that it increases continuously and changes the concavity at the critical point ( $\sigma_c=1$ ), as shown in Fig. 3. This point is also characterized by a rapid change of the curve direction. Depending on the value of  $D$ , we can have second-order ( $D=0.05$  eV) nearly tricritical ( $D=0.1$  eV) or first-order ( $D=0.2$  eV) phase transitions. If  $D$  is less than ca.  $0.1207$ , the reduced temperature  $\chi$  varies monotonically with  $\sigma$  (second-order transition and tricritical at  $D=0.1207$ ), and if  $D$  exceeds this value, single values of  $\chi$  correspond to three  $\sigma$  around the transition point defined by  $\sigma/\sigma_c=1$ . This characterizes the appearance of an abrupt transition from an asymmetric bond to symmetric bond, upon reaching critical temperature, characteristic of the first-order transition. The variance also presents saturation at low temperatures,  $\chi \rightarrow 0$ , showing that quantum fluctuation remains in the quantum regime, while for  $\chi > 1$  the variance  $\sigma$  increases monotonically as  $\chi$  increases.

According to the fact that the barrier height is relevant to the transition mechanism, as deep wells correspond to order-disorder limit while shallow wells are typical for the displacive limit, we investigate the soft mode frequency as a function of barrier height through parameter  $D$ , and typical

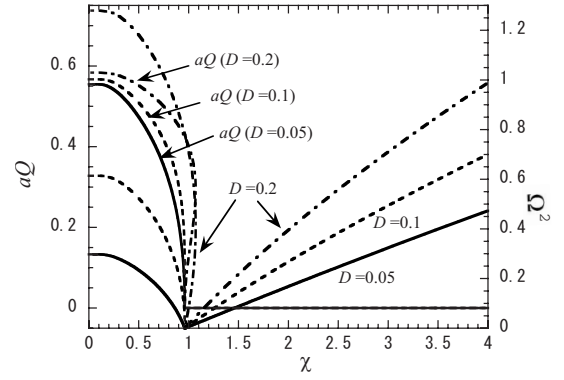


FIG. 4. The spontaneous displacement  $Q$  and the effective frequency  $\Omega$  as function of the normalized temperature  $\chi$ , with parameters  $D=0.05, 0.1$ , and  $0.2$  eV, and  $a=3 \text{ \AA}^{-1}$ ,  $d=0.3 \text{ \AA}$ ,  $v=1.0 \text{ eV/\AA}^2$ , and  $m=50$  amu. If  $D$  exceeds ca.  $0.1207$ , the order parameter indicates the first-order transition. The squared frequency  $\Omega^2$  represents  $[(\Omega/\Omega_0)^2 - 1]/\Delta$  from Eq. (26) as in Fig. 2.

results for the effective frequency as a function of temperature. Also, it appears that the nature of transition is strongly dependent on barrier height, and as  $D$  increases, the transition to the ferroelectric phase takes place and the transition must be second-order, tricritical or first-order phase transition, respectively. Incorporating Figs. 2 and 3, we get temperature dependences of the spontaneous displacement  $Q$  and the effective frequency  $\Omega^2$  as shown in Fig. 4. For small  $D$ , the spontaneous displacement decreases with increasing the reduced temperature  $\chi$  as  $(aQ)^2 \sim (\chi_c - \chi)$  with the second-order transition point  $\chi_c \approx 0.9699$  for the given parameters. When  $D=0.1207$ ,  $Q$  vanishes steeply with indicating tricritical points. For large  $D$ , the spontaneous displacement takes two values in a finite range of  $\chi \geq \chi_c$ ; the transition is the first order one.

In all cases we investigated that the effective frequency saturates at low temperatures by quantum fluctuations and is nearly independent of temperature for a rather broad regime. In the ferroelectric phase, the soft mode rapidly recovers and approaches a temperature independent plateau in the quantum limit, where the soft mode energy depends on the corresponding  $T_c$ , i.e., the larger  $T_c$  the higher is its energy at  $T=0$  K. Simultaneously, in the paraelectric phase, an increase shift in the effective frequency in the higher values of temperature is observed. As can be also seen in Fig. 4, where the temperature dependence of the spontaneous displacement is presented, the quantum fluctuations dominated regime is remarkable, and the quantum fluctuations are not restricted to small temperatures, but can also be presented over an extended temperature regime as they lower the transition temperature. Obviously, according to the value of  $D$  (in the case of first-order phase transitions), we observe that in a slightly limited temperature interval above  $T_c$ , both, the paraelectric and the ferroelectric solutions are simultaneously stable. The coexistence regime depends on the transition temperature and grows with increasing  $D$ .

In order to understand the conditions of appearance of phase transition and its nature, the tricritical lines for different values of the potential splitting parameter  $d$  is presented

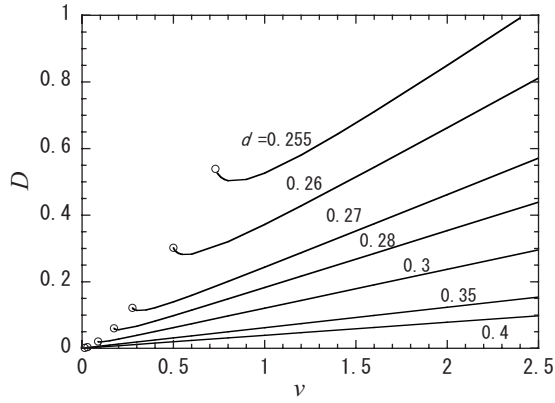


FIG. 5. Tricritical lines where second-order transition changes to a first-order one. If  $D$  exceeds the line for fixed  $d$  and  $v$ , the  $Q$ - $T$  curve has a lip indicating the first-order transition. Each tricritical line terminates at the left end (small open circle), because no phase transition happens for smaller interaction  $v$ .

where the second-order transition changes to a first-order one as shown in Fig. 5. If  $D$  exceeds a tricritical line for fixed  $d$  and  $v$ , the first-order transition takes place, as described in Figs. 3 and 4. Also, the transition at fixed geometry characterized here by parameters  $D$  and  $d$  results in the interaction parameter  $v$ , because no phase transition happens for smaller interaction as can be seen at the left end (small open circle) of each tricritical line in Fig. 5.

These results show important influences of the quantum-mechanical fluctuation enhancement on the behavior of the system, especially at low temperatures. Then, a reduction of the transition temperature due to quantum effects (influences) leads to the following result:

$$T_c = \frac{2v\sigma_c}{k_B} \eta \left/ \ln \frac{1+\eta}{1-\eta} \right. = 2T_0 \eta \left/ \ln \frac{1+\eta}{1-\eta} \right., \quad (28)$$

where

$$T_0 = v\sigma_c/k_B \quad (29)$$

is the classical transition temperature. Equation (28) shows the influence of increasing the involved mass (mass dependence) on transition temperature through the quantum effect magnitude  $\eta$ .

In order to investigate the quantum mechanical influence on the transition mechanism, we plot in Fig. 6 the reduction of the transition temperature against the measure of the quantum influence. It appears that the transition temperature decreases continuously with the quantum influence. Thus, the quantum effect lowers the transition temperature, which shows the large influence of quantum effect on the mechanism and nature of the phase transition.

From (9), (27), and (29), we can define another characteristic temperature,

$$T_1 = 2\eta T_0 = 2\theta_s, \quad (30)$$

and (28) is reduced to

$$T_c = T_1 \left/ \ln \frac{T_0 + T_1/2}{T_0 - T_1/2} \right. \quad (31)$$

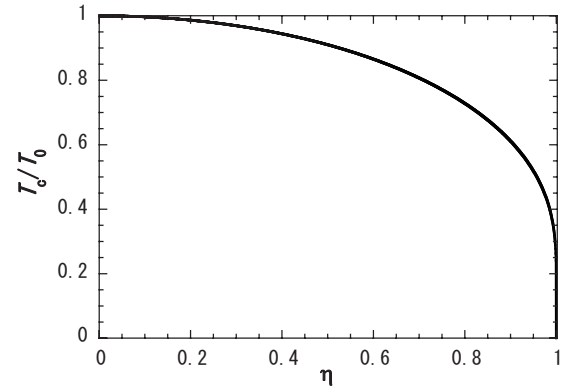


FIG. 6. The quantum parameter  $\eta$  dependence on the transition temperature  $T_c$  from Eq. (28).

Equation (31) is in agreement with that obtained from the Barrett formula (equation) for the dielectric constant (or static susceptibility),<sup>24,38,39</sup> except that the characteristic parameters  $T_1$  and  $T_0$  are expressed in terms of different physical quantities.  $T_1$  may also yield useful insights into the behavior of the phase transitions and it seems that  $T_1$  is not greatly altered by chemical doping or application of external fields. This presents the influence of the quantum mechanical effects on the transition particularly on the transition temperature, and is related to the experimental evidence which seems to support the dominance of the softening of optic branches so that the Einstein mode approximation appears to be appropriate for ferroelectrics and most improper ferroelastics phase transitions. The structural phase transition takes place when the interaction is strong enough:  $T_0 > T_1/2$ , so that phase transitions cannot be suppressed by quantum fluctuations which dominate the system [see Eq. (22)] and then the system undergoes a ferroelectric transition.

The zero-point fluctuations with variance  $\sigma_s$  give rise to a reduction of the order parameter  $Q_s$  at zero temperature as compared to its classical value  $Q_0$ , given by

$$\frac{Q_s}{Q_0} = \frac{\cosh^{-1} \left[ \frac{1}{2} e^{ad} \exp(-1.5a^2\sigma_s) \right]}{\cosh^{-1} \left( \frac{1}{2} e^{ad} \right)}. \quad (32)$$

The value of  $\sigma_s$  is then determined by the solution of the following equation:

$$\frac{\sigma_s}{\sigma_c} \sqrt{1 + \Delta [\exp(-a^2\sigma_s) - 4e^{-2ad} \exp(2a^2\sigma_s)]} = \eta, \quad (33)$$

which follows from the self-consistency Eqs. (25) and (26) for  $T=0$ .

Thus, Fig. 1 presents the effective potentials for different values of  $\sigma/\sigma_c$  between 0.5 and 2. For this figure, the other model parameters are taken to be  $a=3 \text{ \AA}^{-1}$  and  $d=0.3 \text{ \AA}$ . This suggests that quantum fluctuations tend to displace the particles (atoms) from the classical potential minima towards their respective reference lattice sites. According to this, the minima of the effective potential shifts towards the origin as  $\sigma/\sigma_c$  increases, which means that the model takes analytically into account the possibility to shift the potential minima

(backbones flexibility of molecular solids that chemical bonds must continuously relax or contract to avoid bond breaking). Also, according to the effective potential profiles, the particles quantized below their barrier are able to tunnel. We can therefore conclude that the experimentally observed double occupancy in the H bridges should be ascribed to the correlated dynamics of heavy atoms or clusters involving heavy surrounding atom displacements and that the proton tunneling is essential in the proton system with a double minimum potential.

#### IV. KDP-TYPE PHASE DIAGRAM

The two Morse potential has also been applied for KDP and DKDP previously and different values of model parameters have been proposed. For example, Matsushita and Matsubara have estimated  $d$  as 0.27 for KDP and 0.28 Å for DKDP.<sup>26</sup> Sugimoto and Ikeda estimated  $d=0.30$  and 0.31 Å for KDP and DKDP, respectively.<sup>40</sup> Mashiyama has also assigned  $d=0.27$  and 0.28 Å for KDP and DKDP, respectively, in order to reproduce the nuclear density distribution (determined from neutron diffraction measurement) on the one hand,<sup>24</sup> and has adopted  $d=0.295$  Å for both proton and deuteron to stress the tunneling effect clearly on the other hand.<sup>41</sup> Also, in the paraelectric phase of KDP, the neutron diffraction analysis revealed a double-peak density distribution of the hydrogen: the peak splitting was reported as 0.32 and 0.44 Å for KDP and DKDP, respectively.<sup>42</sup>

In what follows, and in order to model well the hydrogen bonds and investigate the transition of the proton-tunneling system in KDP, our assignment for  $d$  is 0.29 Å for KDP. Also, according to experimental results and in order to reproduce them, the following model parameters are selected to be  $a=3$  Å<sup>-1</sup>,  $D=0.05$  eV, and  $v=0.85$  eV/Å<sup>2</sup>. The saturation temperature is estimated as  $\theta_s=41.75$  K for KDP in agreement with the value determined by fitting the experimental data from Samara and Nelmes *et al.*<sup>43,44</sup> Then, the potential minimum is 0.21 Å. These values are in agreement with those previously estimated,<sup>24–26,40</sup> although the parameter  $D$  is smaller than the expected previous values, i.e., the potential barrier is smaller. The value of  $D$  is adopted also in order to stress the tunneling effect clearly and especially in KDP.

Here it should be noted that the effective mass of KDP is about 46.55 amu from Eq. (9), which corresponds to one-half of the bare mass of the H<sub>2</sub>PO<sub>4</sub> molecule confirming the fact that reorientation of an H<sub>2</sub>PO<sub>4</sub> dipole means the distortion,<sup>45,46</sup> and that the relative displacement between the P and O atoms is the dominant factor.<sup>4</sup> Also, the interaction between proton and PO<sub>4</sub> is only considered through the effective interaction between normal coordinates of the ferro-distortive mode. This means we are dealing with not an isolated hydrogen but the H<sub>2</sub>PO<sub>4</sub> molecular effectively. Thus, H bridges should be ascribed to the correlated dynamics of heavy clusters involving P and K displacements and large clusters as recently shown by *ab initio* calculations.<sup>4,19</sup> Then, the normal local coordinate in this system is considered to be due to the cooperative motion of two protons and the quasi-rotation of PO<sub>4</sub> tetrahedra.<sup>47,48</sup> Also, the potential barrier disappears if  $d<0.231$  Å. In order to examine the huge iso-

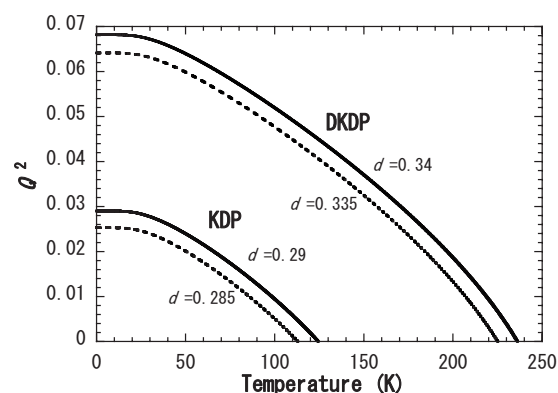


FIG. 7. Temperature dependence of the squared order parameter  $Q^2$  for both KDP and DKDP and for two different values of  $d$ . Parameters are given by  $a=3.0$  Å<sup>-1</sup>,  $D=0.05$  eV,  $v=0.85$  eV/Å<sup>2</sup>,  $\theta_s=41.75$  K,  $d=0.285$ , and 0.29 Å for KDP, while  $\theta_s=41.25$  K,  $d=0.335$ , and 0.34 Å for DKDP at atmospheric pressure.

tope effect, we reported  $d$  around 0.34 Å and according to the mass dependence of quantum effects, we estimated  $\theta_s=41.25$  K for DKDP. The potential minimum is around 0.27 Å, and the effective mass is 48.55 amu, which is also equal to one-half of the D<sub>2</sub>PO<sub>4</sub> molecule's bare mass. Also, the cluster tunneling is allowed for with effective mass much larger than the total involved H or D mass, and large ones are clearly relevant for the nearly second-order ferroelectric transition in the KDP system.<sup>49</sup> These model parameters are also chosen so that the  $T_c$  for the deuteron system is about 100 K higher than that for the proton and agree well with previous work.<sup>24–26,40,41</sup>

Figure 7 shows the temperature dependences of the squared order parameter of both KDP and DKDP systems along the ferroelectric  $c$  axis at atmospheric pressure. Here also, the quantum saturation of the order parameter at low temperatures can be recognized which confirms the domination of quantum effects at low temperature. Then, the calculated transition temperatures are estimated about  $T_c \approx 124.5$  K for KDP and  $T_c \approx 236.2$  K for DKDP. These values are in the same order with the well-known experimental values and in satisfactory agreement.

We conclude that most of this effect arises from the modification of the H-bridge length due to a larger quantum delocalization of H than D, thus leading to a stronger covalent binding of the bridged oxygens in KDP. However, obviously, the main contribution arises from the geometric changes of hydrogen bonds through the lattice parameter  $d$  which affects the covalency of the bonds. Thus, our calculations show that the simple change of mass upon deuteration at fixed geometry does not explain the almost duplication of  $T_c$ .

Let us begin by showing the influence of model parameters on the transition phenomenon in KDP crystals. In fact, we demonstrate the transition temperature  $T_c$  as function of  $d$  and  $v$ . Figures 8 and 9 plot how  $T_c$  changes with the interaction parameter  $v$  and splitting distance  $d$ , respectively, and for KDP and DKDP. Thus, with decreasing  $d$  or  $v$ ,  $T_c$  decreases monotonically. Then, the decrease of  $T_c$  as  $d$  decreases is due to the potential minimum becoming shallow and the potential barrier low. In addition, strong interaction  $v$  or  $d$ , higher is transition temperature.



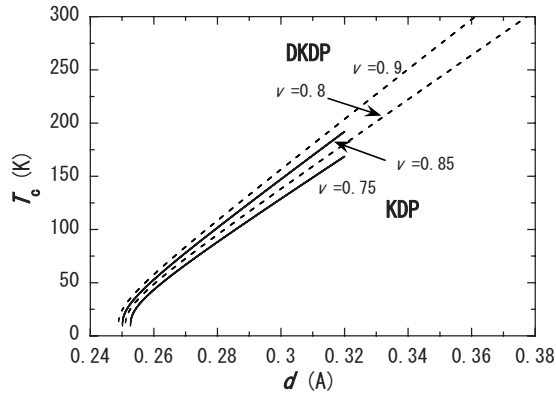


FIG. 8. Transition temperature as a function of  $d$  with different  $v$  values. The solid and broken curves represent  $T_c$  for KDP and DKDP, respectively. Parameters are  $a=3.0 \text{ \AA}^{-1}$ ,  $D=0.05 \text{ eV}$ ; and  $v$  is 0.75 and 0.85  $\text{eV/\AA}^2$ , and the saturation temperature  $\theta_s=41.75 \text{ K}$  for KDP while  $v$  is 0.8 and 0.9  $\text{eV/\AA}^2$  and  $\theta_s=41.25 \text{ K}$  for DKDP.

For fixed  $v(d)$  with decreasing  $d(v)$ ,  $T_c$  is rapidly depressed and the ferroelectric instability vanishes at some critical value of  $d(v)$  which decreases (increases) with  $v(d)$  as shown in Figs. 8 and 9, respectively, for both KDP and DKDP. Also from Fig. 8, under some conditions such as applying pressure to DKDP in such an amount that the value of splitting parameter  $d$  is turned to its value in KDP at normal pressure, the value of  $T_c$  in DKDP is brought almost to coincidence with the one of KDP, in spite of the mass difference between H and D. However for the values close to critical  $d$ , the variation is too small.

Thus, mass change due to deuteration at fixed structural parameters cannot account for the huge isotope effect. With the substantial change in the geometric characteristics as size, potential barrier, effective mass, through the splitting potential parameter, which are lattice parameters, the isotope effect on  $T_c$  appears: this is the so-called geometrical effect, and is shown in Fig. 9. As defined, an alternative strategy to investigate the structure of the ferroelectric phase transition

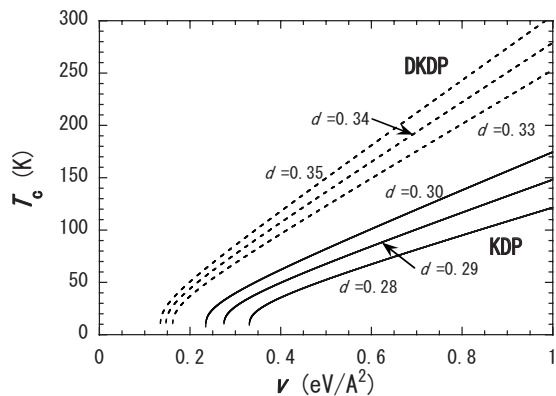


FIG. 9. Transition temperature as a function of  $v$  with three  $d$ 's (0.28, 0.29, and 0.30  $\text{\AA}$  for KDP; 0.33, 0.34, and 0.35  $\text{\AA}$  for DKDP). Other parameters are chosen as  $a=3.0 \text{ \AA}^{-1}$ ,  $D=0.05 \text{ eV}$ ,  $v=0.85 \text{ eV/\AA}^2$  and the saturation temperature  $\theta_s=41.75 \text{ K}$  for KDP while  $\theta_s=41.25 \text{ K}$  for DKDP.

is to analyze its thermodynamic behaviors and also phase diagrams. In a crystal, protons or deuterons interact with each other directly or indirectly, and an ordered state can be realized at finite temperature. Also, it has been recognized that the shape of the potential along the H bond is strongly dependent on the length of the bond and since the H bond is mechanically the weakest link in the crystal structure, the properties of these crystals can be expected to be strongly pressure dependent.

Because many crystal lattices reduce their sizes under hydrostatic pressure and it has been observed that the oxygen-oxygen distance of KDP shrinks and the proton distribution becomes single peaked at high pressure, we will assume that some model parameters are pressure dependent. In order to model the phase diagram, it is necessary to consider how the parameters will be affected by changes in pressure. The pressure dependences of quantities  $T_0$  and  $T_1$  provide us with the useful information to discuss qualitatively the dependences of microscopic parameters on  $p$  if compared with their definitions derived from the Hamiltonian given in Eq. (1). Here, we will assume that the potential splitting  $d$  and the interaction strength  $v$ , respectively, decreases and increases on applying pressure. This plausible assumption takes into account the fact that pressure makes the lattice shrink which would shorten the O-O distance to decrease  $d$  and would also shorten the neighboring distance between protons and may increase the interaction. Also, since the H(D) bond is mechanically the weakest link in the crystal structure, the properties of these crystals can be expected to be strongly pressure dependent. According to all this, some experimental results, the decrease of  $T_0$  with increasing pressure and pressure dependence of some model parameters of KDP and DKDP, we adopt the following pressure dependence on  $d$  and  $v$ ,

$$d = 0.29 - 0.017p \quad \text{and} \quad v = 0.85 + 0.005p \quad (34)$$

for KDP and,

$$d = 0.34 - 0.017p \quad \text{and} \quad v = 0.85 + 0.005p \quad (35)$$

for DKDP. Here  $p$  is in units of GPa, and  $d$  and  $v$  in  $\text{\AA}$  and  $\text{eV/\AA}^2$ , respectively. This supposition also shows the qualitative agreement with the fact that the decrease of  $T_c$  should be attributed to the decrease of  $T_0$  at  $p < p_c$  contrary to the naive tunneling model.<sup>46</sup> Then, their corresponding pressure-temperature phase diagrams are reproduced as shown in Fig. 10. In both cases, the transition temperature  $T_c$  decreases monotonically with increasing pressure to vanish at critical pressure  $p_c$  owing to the quantum effect characterized by the Einstein temperature  $T_1$  at  $p \geq p_c$ . The calculated phase diagram is in agreement qualitatively with the experimental one, both in KDP and DKDP.<sup>50,51</sup> Though the vanishing of the ferroelectric state has been observed at  $p_c=2.36 \text{ GPa}$  and  $p_c=5.54 \text{ GPa}$  for KDP and DKDP, respectively. These values can be compared to the experimental critical pressure values 1.7 GPa (KDP)<sup>50</sup> and 6.3 GPa (DKDP),<sup>51</sup> above which no phase transition takes place, or 1.3 GPa (KDP) and 5.8 GPa (DKDP), from measurement of the dielectric constant and analysis of experimental data to fit the Barrett equation under high pressure.<sup>46</sup>

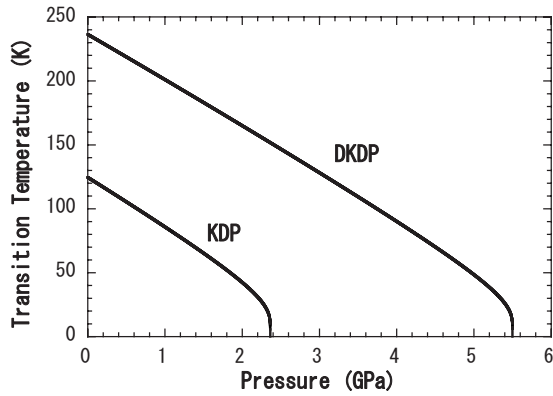


FIG. 10. Pressure dependence of the transition temperature for KDP and DKDP. Parameters are  $a=3.0 \text{ \AA}^{-1}$ ,  $D=0.05 \text{ eV}$ ,  $v=0.85 + 0.005p \text{ eV/\AA}^2$ , and  $\theta_s=41.75 \text{ K}$  and  $d=0.29-0.017p \text{ \AA}$  for KDP, while,  $\theta_s=41.25 \text{ K}$  and  $d=0.34-0.017p \text{ \AA}$  for DKDP.

### V. SUMMARY

According to this study, our simple model is successful qualitatively to describe a structural ferroelectric phase transition, and phase diagram due to an appropriate pressure dependence of transition temperature  $T_c$ . Also the quantum effects are important if the transition takes place at low temperature. The ferroelectric localized distortions involving also heavy atoms do exhibit double wells, whose ground state lies below the barrier; thus allowing tunneling. In KDP systems, however, quantum mechanically, the proton becomes much more delocalized than the deuteron, and finds itself more often than the latter between the oxygens. This favors covalent bonding between them, therefore pulling the oxygens together, and shrinking the lattice. Thus, our calculations show that the simple change of mass upon deuteration at fixed geometry does not explain the near duplication of  $T_c$ , as the variation of the tunnel splitting in large clusters accounts only for small variation of  $T_c$ . According to our results, and from Fig. 9, the model parameters characteristics like size, barriers, and effective masses, are quite different in KDP and DKDP, a fact which is self-consistently related to their lattice parameters, and which is in accordance with the recent *ab initio* results and the tunneling clusters models.<sup>19,52</sup> These results confirm the important role of the heavy-atoms dynamics in the  $\text{PO}_4\text{-K}$  group to produce significant instabilities of the local proton (deuteron) distortions with the ferrodistorptive mode pattern,<sup>4,19,52</sup> and that it is the geometrical changes upon isotopic substitution of proton by deuteron (deuteration) the principal mechanism responsible for the huge isotope effect.<sup>19,44,52</sup> This also clarifies the physical reason leading to a larger lattice parameter in DKDP than in KDP, in agreement with neutron scattering experiments.<sup>44</sup>

The pseudo-Barrett equation obtained confirms the important role of Barrett equation in the investigation of theory of ferroelectric phase transition which fitted well some experimental data. The temperature evolution of variance  $\sigma$  is determined in the displacive limit by the dispersion relations of the coupled branches, but experimental evidence seems to support the dominance of the softening of optic phonon branches so that the Einstein mode approximation appears to

be appropriate for ferroelectric and most improper ferroelastic phase transitions.<sup>33,36,53</sup>

In Fig. 7, the temperature dependence of the order parameter shows the quantum saturation of the order parameter in both KDP and DKDP at low temperatures in accordance with the third law of thermodynamics. At  $T \leq \theta_s$ , the saturation sets in and the value  $Q_s$  is reached, showing the domination of the quantum mechanical effects. Also, the transitions for both cases are thermodynamically close to the displacive limit and nearly tricritical, respectively, which seems to be qualitatively in accordance with the evidence of existence of the displacive component (character) in  $\text{KH}_2\text{PO}_4$  phase transition mechanism performed by molecular simulation (MD),<sup>54</sup> *ab initio* calculations,<sup>4</sup> and which was previously observed experimentally on the one hand, and also in agreement with the microscopic evidence indicating that phase transitions in crystals of the KDP group must be close to the tricritical point,<sup>53,55</sup> and detected nearly tricritical transition (point) in  $\text{KH}_2\text{PO}_4$  crystal using  $\gamma$ -ray diffraction,<sup>56</sup> on the other hand.

Amongst other things, the ratio  $T_c^D/T_c^H$  is estimated to be around 1.89 compared to the observed one at 1.75. Moreover,  $T_0$  decreases with increasing pressure and  $T_1$  remains constant, which agrees well with the recent study of Endo *et al.* which measured the dielectric constant  $\epsilon_c$  along the ferroelectric axis of KDP and DKDP under high pressure.<sup>46</sup> They analyzed the experimental data to fit the Barrett equation and found that  $T_0$  decreases with increasing pressure and  $T_1$  is almost constant. This is also confirmed by Fig. 9. According to this, the characteristics of the phase transition depend on the model parameters  $D$ ,  $a$ , and  $d$ , in Eq. (2), as well as the interaction parameter  $v$  but also on the saturation temperature  $\theta_s$ ; confirming the fact that,  $\theta_s$  may actually be a more useful parameter for characterizing phase transitions than  $T_c$ , in spite of an understanding of the principle which determines what is  $\theta_s$  for a given phase transition.<sup>36,57</sup> If the transition takes place at low temperature, the quantum effect is important; therefore,  $T_c$  vanishes logarithmically as shown by Figs. 8 and 9. However, below some critical values of  $d$  and  $v$ , no phase transition takes place. When the interaction parameter with protons is the same as that with deuterons, the lattice with protons always has a lower transition temperature  $T_c$  than with deuterons.

Furthermore, from Figs. 8 and 9, it appears that the increase of  $T_c$  cannot be more than several tens of a degree in the model if deuteration does not cause any change in lattice parameters. We have estimated the pressure dependence of model parameters  $d$  and  $v$  (from experimental results) and calculated the transition temperature of our model as a function of pressure. When the pressure is applied,  $d$  decreases whereas  $v$  increases, or simultaneously  $v\sigma_c$  decreases even if  $v$  increases, the transition temperature is lowered and finally the transition itself vanishes at certain magnitude of pressure as shown in Fig. 10. Thus, the calculated pressure-temperature phase diagrams for KDP and DKDP follow qualitatively the experimental (real) phase diagrams obtained for KDP system by Samara,<sup>43,50</sup> and for DKDP system by Endo *et al.*<sup>51</sup>

The steep decreasing of  $T_c$  around  $p_c$  is also the quantum effect in fact that  $dT_c/dp$  should tend to  $-\infty$  at  $T=0$  accord-

ing to the third law of thermodynamics. Amongst other things is the large isotope effect because ferroelectric state vanishes in DKDP at a pressure over threefold than in KDP. In this figure, only  $d$  and  $v$  are fitted parameters. The other Morse potential parameters are fixed. Then, a slight change of the model parameters of the Hamiltonian brings about a substantial change in the thermodynamic picture of the phase transition.

Moreover, Fig. 6 which presents the dependence of quantum influence on transition temperature  $T_c$  as compared to its classical value, shows that, although the proton tunneling is essential in the proton (deuteron) system with double minimum potential, the decrease of  $T_c$  should be explained on the basis of quantum effects other than the tunneling model. The mechanism of ordering of protons on hydrogen bonds appears as the principal mechanism leading to the spontaneous

polarization in the KDP-type crystals. We can then conclude that our model presents useful information to discuss qualitatively the dependences of microscopic parameters on pressure and our assumption is in agreement with the hard change of  $T_1$  [see Eq. (30)] and the unexpected decrease of effective interaction defined by  $T_0$  [see Eq. (29)], with increasing pressure, obtained experimentally for KDP under high pressure by Endo *et al.*<sup>46</sup>

#### ACKNOWLEDGMENTS

One of the authors (S.E.M.T.) is grateful for the full support from the Ministry of Education, Science and Culture of Japan through MONBUKAGAKUSHO, and Yamaguchi University, where the work was performed.

\*Electronic address: h501hr@yamaguchi-u.ac.jp

- <sup>1</sup>M. E. Lines and A. M. Glass, *Principles and Applications of Ferroelectrics and Related Materials* (Clarendon, Oxford, 1977).
- <sup>2</sup>J. C. Slater, *J. Chem. Phys.* **9**, 16 (1941); C. C. Stephenson and J. F. Hooley, *J. Am. Chem. Soc.* **66**, 1397 (1944).
- <sup>3</sup>R. A. Cowley, *Adv. Phys.* **29**, 1 (1980).
- <sup>4</sup>Q. Zhang, N. Kioussis, S. G. Demos, and H. B. Radousky, *J. Phys.: Condens. Matter* **14**, L89 (2002).
- <sup>5</sup>J. A. Krumhansl and J. R. Schrieffer, *Phys. Rev. B* **11**, 3535 (1975).
- <sup>6</sup>Y. Yacoby, B. Rechaw, N. Sicron, E. A. Stern, J. J. Rehr, and B. Ravel, *Physica B* **208-209**, 259 (1995).
- <sup>7</sup>A. D. Bruce, *Adv. Phys.* **29**, 111 (1980).
- <sup>8</sup>S. Aubry, *J. Chem. Phys.* **62**, 3217 (1975).
- <sup>9</sup>T. Mitsui, I. Tatsuzaki, and E. Nakamura, *An Introduction to the Physics of Ferroelectrics* (Gordon and Breach, New York, 1976).
- <sup>10</sup>M. Tokunaga, *J. Phys. Soc. Jpn.* **57**, 4275 (1988).
- <sup>11</sup>Y. Onodera and N. Kojyo, *J. Phys. Soc. Jpn.* **58**, 3227 (1989).
- <sup>12</sup>W. Cochran, *Adv. Phys.* **9**, 387 (1960).
- <sup>13</sup>Y. Nakajima and S. Naya, *J. Phys. Soc. Jpn.* **63**, 3619 (1994).
- <sup>14</sup>E. K. H. Salje, B. Wruck, and H. Thomas, *Z. Phys. B: Condens. Matter* **82**, 399 (1991).
- <sup>15</sup>P. G. de Gennes, *Solid State Commun.* **1**, 132 (1963).
- <sup>16</sup>Y. Onodera, *Prog. Theor. Phys.* **44**, 1477 (1970); **45**, 986 (1971).
- <sup>17</sup>J. M. Pérez-Mato and E. K. H. Salje, *J. Phys.: Condens. Matter* **12**, L29 (2000).
- <sup>18</sup>G. Busch and P. Scherrer, *Naturwiss.* **23**, 737 (1935).
- <sup>19</sup>S. Koval, J. Kohanoff, R. L. Migoni, and E. Tosatti, *Phys. Rev. Lett.* **89**, 187602 (2002).
- <sup>20</sup>M. Tokunaga and T. Matsubara, *Ferroelectrics* **72**, 175 (1987).
- <sup>21</sup>M. Tokunaga and I. Tatsuzaki, *Phase Transitions* **4**, 97 (1984).
- <sup>22</sup>R. Blinc, *J. Phys. Chem.* **13**, 204 (1960).
- <sup>23</sup>K. K. Kobayashi, *J. Phys. Soc. Jpn.* **24**, 497 (1968).
- <sup>24</sup>H. Mashiyama, *J. Korean Phys. Soc.* **46**, 63 (2005).
- <sup>25</sup>M. C. Lawrence and G. N. Robertson, *Ferroelectrics* **34**, 179 (1981).
- <sup>26</sup>E. Matsushita and T. Matsubara, *Prog. Theor. Phys.* **67**, 1 (1982).
- <sup>27</sup>A. M. Dikande and T. C. Kofane, *J. Phys.: Condens. Matter* **3**, 5203 (1991); A. M. Dikande and T. C. Kofane, *Solid State Commun.* **89**, 559 (1994).
- <sup>28</sup>G. Kalosakas, A. V. Zolotaryuk, G. P. Tsironis, and E. N. Economou, *Phys. Rev. E* **56**, 1088 (1997).
- <sup>29</sup>P. Tchofo Dinda, *Phys. Rev. B* **46**, 12012 (1992).
- <sup>30</sup>S. A. Hayward and E. K. H. Salje, *J. Phys.: Condens. Matter* **10**, 1421 (1998).
- <sup>31</sup>O. Yanovitskii, G. Vlastou-Tsinganos, and N. Flytzanis, *Phys. Rev. B* **48**, 12645 (1993).
- <sup>32</sup>H. Thomas, in *Structural Phase Transitions and Soft Modes*, edited by E. J. Samuelson, E. Andersen, and J. Feder (Universitetsforlaget, Oslo, 1971).
- <sup>33</sup>E. K. H. Salje, in *Quantum Saturation of the Spontaneous Polarization in Ferroelectric Materials: Fundamental Physics of Ferroelectrics*, edited by R. E. Cohen (American Institute of Physics, New York, 2000), p. 297.
- <sup>34</sup>M. Peyrard, St. Pnevmatikos, and N. Flytzanis, *Phys. Rev. A* **36**, 903 (1987).
- <sup>35</sup>J. Y. Lee and K. L. Liu, *Physica A* **286**, 573 (2000).
- <sup>36</sup>S. A. Hayward, S. A. T. Redfern, and E. K. H. Salje, *J. Phys.: Condens. Matter* **14**, 10131 (2002).
- <sup>37</sup>E. K. H. Salje, B. Wruck, and S. Marais, *Ferroelectrics* **124**, 185 (1991).
- <sup>38</sup>J. H. Barrett, *Phys. Rev.* **86**, 118 (1952).
- <sup>39</sup>K. A. Müller and H. Burkard, *Phys. Rev. B* **19**, 3593 (1979).
- <sup>40</sup>H. Sugimoto and S. Ikeda, *Phys. Rev. Lett.* **67**, 1306 (1991).
- <sup>41</sup>H. Mashiyama, *J. Phys. Soc. Jpn.* **73**, 63 (2004).
- <sup>42</sup>R. J. Nelmes, G. M. Meyer, and J. E. Tibballs, *J. Phys. C* **15**, 59 (1982).
- <sup>43</sup>G. A. Samara, *Phys. Rev. Lett.* **27**, 103 (1971).
- <sup>44</sup>R. J. Nelmes, M. I. McMahon, R. O. Piltz, and N. G. Wright, *Ferroelectrics* **124**, 355 (1991).
- <sup>45</sup>E. A. Popova and D. S. Bystrov, *Ferroelectrics* **72**, 45 (1987).
- <sup>46</sup>S. Endo, K. Deguchi, and M. Tokunaga, *Phys. Rev. Lett.* **88**, 035503 (2002).
- <sup>47</sup>Y. Tominaga, H. Urabe, and M. Tokunaga, *Solid State Commun.* **48**, 265 (1983).
- <sup>48</sup>M. Ichikawa, K. Motida, and N. Yamada, *Phys. Rev. B* **36**, 874

- (1987).
- <sup>49</sup>G. A. Samara, *Ferroelectrics* **5**, 25 (1973).
- <sup>50</sup>G. A. Samara, *Ferroelectrics* **7**, 221 (1974).
- <sup>51</sup>S. Endo, T. Sawada, T. Tsukawake, Y. Kobayashi, M. Ishizuka, K. Deguchi, and M. Tokunaga, *Solid State Commun.* **112**, 655 (1999).
- <sup>52</sup>S. Koval, J. Kohanoff, J. Lasave, G. Colizzi, and R. L. Migoni, *Phys. Rev. B* **71**, 184102 (2005).
- <sup>53</sup>B. A. Strukov and A. P. Levanyuk, *Ferroelectric Phenomena in Crystals: Physical Foundations* (Springer-Verlag, Berlin, Heidelberg, New York, 1998).
- <sup>54</sup>D. Merunka and B. Rakvin, *Solid State Commun.* **129**, 375 (2004).
- <sup>55</sup>A. N. Zisman, V. N. Kachinkii, and S. M. Stishov, *Pis'ma Zh. Eksp. Teor. Fiz.* **31**, 172 (1980).
- <sup>56</sup>P. Bastie and P. Becker, *J. Phys. C* **17**, 193 (1984).
- <sup>57</sup>J. M. Pérez-Mato and E. K. H. Salje, *Philos. Mag. Lett.* **81**, 885 (2001).